The obtaining of titanium dioxide nanocrystalline powders

A. MOLEA, V. POPESCU[a,*]
Technical University of Cluj-Napoca, Cluj-Napoca, Romania
[a]*Technical University of Cluj-Napoca, Cluj-Napoca, Romania*

The paper describes the obtaining of TiO_2 nanocrystalline powders by sol-gel method. TiO_2 nanocrystalline powder was obtained by hydrolysis of $TiCl_3$ precursors in alkaline medium. The influence of bath condition (static or magnetic stirring), treatment with concentrated H_2O_2 and thermal treatment at 500 ^oC for one hour was investigated. In the absence of H_2O_2 a crystalline phase containing both anatase and rutile has been obtained, while in the case of oxidized sample anatase alone has been identified. Structural analyses were made using X ray diffraction. Optical properties have been determined using UV-VIS spectroscopy. The band gap of the obtained powder has been calculated. Thermal treatment and H_2O_2 oxidation leads to the red shift of the band gap energy for all samples. The photoresponse of all samples moved from ultraviolet to visible region. The obtained powder can be embedded in a polymer matrix, in order to obtain photoactive composite materials.

(Received March 7, 2011; accepted March 16, 2011)

Keywords: Titanium dioxide, Nanocrystalline powder, Sol-gel method, $TiCl_3$ precursors, Semiconductor, UV-Vis spectroscopy, X ray diffraction

1. Introduction

Titanium dioxide is a semiconductor widely studied because of his special properties, such as photocatalytic property [1,2]. Titanium dioxide has the ability to decompose water and air pollutants under ultraviolet radiation by absorbing the radiation and sparking a series of photochemical reactions. Bulk anatase TiO_2 has the energy band gap 3.2 eV while rutile has a band gap value of 3 eV. To absorb in visible region, the energy band gap of TiO_2 must be in the range of 1.4 to 3 eV (corresponding to solar spectrum).

Nanostructured titanium dioxide can be obtained by chemical methods: sol-gel [3,4], chemical bath deposition [5,6], chemical vapour deposition [7,8] and physical methods such as physical vapour deposition [9]. TiO_2 film or powder was obtained by chemical methods using as precursor $TiCl_3$ [10-12]. Thus, Lee et al [10] obtained TiO_2 film by the immersion of different substrates into peroxo titanic acid solution. Cassaignon et al [12] synthesized TiO_2 nanoparticles (anatase, brookite and rutile) by thermohydrolysis and oxidation in aqueous medium, thus studying the influence of pH on the crystalline phases and morphology. Through hydrothermal process, Castro et al [11] synthesized anatase TiO_2 nanopowder, crystallization precursor was done in an autoclave. Influence of heat treatment on crystalline phase was studied.

Since the titanium dioxide powder has limitations regarding its application in photocatalytic systems using solar energy, several methods of obtaining composite materials based on titanium dioxide were developed. The optical response of those composites was shifted from UV to visible region. TiO_2/polimer composites can be obtained by dispersing nanostructured titanium dioxide powder in monomer, followed by polymerization, or by dispersing nanostructured powder into melted polymer matrix [13-19]. Another method of obtaining TiO_2 based composites is the deposition of titanium dioxide film on polymer substrate.

Displacement of optical response from UV to visible of TiO_2, can also be achieved through doping TiO_2 with metals and nonmetals [20-24]. Thus, by doping with cadmium, Andronic et al [20] obtained a decreased energy band gap from 3.2 eV for pure TiO_2, to 2.95 eV for TiO_2 doped with cadmium. When doping with nitrogen, Li et al [23] shifted optical response from 3.1 eV for pure TiO_2 to 2.2 eV for $TiO_{2-x}N_x$. Long et al [24] prepared a chlorine-doped titanium dioxide catalyst by hydrolysis of tetrabutyl titanate in hydrochloric acid. Author [24] showed the photocatalytic activity of chlorine-doped TiO_2 catalyst by degradation of phenol under visible light.

This paper describes the obtaining of titanium dioxide powder by sol-gel method, using titanium trichloride $TiCl_3$ as precursor. Oxidation process was accelerated using hydrogen peroxide, for one of the samples. TiO_2 powders were obtained both in static bath and under magnetic stirring. The pH was adjusted to 8 in order to obtain anatase phase of TiO_2. The mechanism of chemical reactions was proposed by Zhang et al [25]:

$$Ti^{3+} + H_2O \rightarrow TiOH^{2+} + H^+$$

$$TiOH^{2+} + O_2 \rightarrow \text{Ti (IV) oxy species} + O_2^- \rightarrow TiO_2$$

In our case the general reaction was:

$$2TiCl_3 + HCl + 7NH_4OH + H_2O + 1/2O_2 \rightarrow 2Ti(OH)_4 + 7NH_4Cl + H_2O$$

$$Ti(OH)_4 \rightarrow TiO_2 + 2H_2O$$

2. Experimental

2.1. Preparation

The deposition solution was prepared using 5 ml of titanium chloride III ($TiCl_3$) 10 %, containing 15 % HCl (Merck), 5 ml distilled H_2O for hydrolysis. A volume of 10 ml NH_4OH (Microchim) was added under continuous stirring in order to obtain alkaline pH. Finally 10 ml hydrogen peroxide 3% was added for the increasing of the oxidation rate. While adding ammonium hydroxide the formation of a dark blue precipitate was observed. The solution obtained was divided into three samples: sample A_1 was obtained in a static bath for 24 h, sample A_2 was obtained by treatment with concentrated H_2O_2 for rapid oxidation and sample A_3 was subjected to magnetical stirring for 24 h (see Table 1). The precipitates obtained as samples A_1 and A_3 was vigorously washed with distilled water several times for removing the impurities (ammonia and chlorine ions) and then the obtained precipitate was filtered in a ceramic filter crucible with a vacuum pump. The precipitate treated with 30 % hydrogen peroxide (sample A_3) was left for a few days for aging in order to form a gel. After the gel was formed it was subjected to heat treatment at 500 ^{0}C for 1h. Samples A_1 and A_3 have been subjected to thermal treatment in the same conditions.

2.2. Characterization of powder

XRD measurements were performed using a XRD-6000 Shimadzu diffractometer, with a monochromator of graphite, for the CuKα radiation operating in the reflection mode between 10–60^0 (2θ). The particle sizes of the nanocrystalline powder were calculated using the Debye-Scherrer's equation:

$$d = \frac{k \cdot \lambda}{B \cdot \cos \Theta} \quad (1)$$

Where: k - particle shape factor; k = 0.9; λ - wavelength of CuKα radiation, λ = 1.54056 [Å]; B - the full width half maximum of the peak [radian]; θ – Bragg's diffraction angle [degree].

The absorbance of suspensions containing TiO_2 powders was measured using a UV-Visible LAMBDA 35 spectrometer. The measurements were taken in a wavelength range of 200–1100 nm.

3. Results and discussion

The synthesis conditions of the TiO_2 samples were listed in Table 1.

Table 1. Synthesis condition of TiO_2 samples.

Sample	Synthesis conditions	Crystallite size* (nm)
A_1	Static at room temperature	13.51
A_2	Treatment with hydrogen peroxide 30%	9.21
A_3	Magnetic stirring for 24h, 340 rpm/min	13.91

Note: * crystallites size was calculated with Debye-Scherrer's equation.

3.1. X-ray diffraction

The XRD patterns of the titanium dioxide particles obtained by sol-gel method are presented in Fig. 1. The peak at 2θ = 25.18 ^{0} (101), 2θ = 37.76^0 (004), 2θ = 47.8 (200), 2θ = 55.06 (211) was assigned to anatase crystalline phase of titanium dioxide and the peak at 2θ = 27.08 (110), 2θ = 35.82^0 (101), 2θ = 41.24^0 (111), was attributed to rutile crystalline phase. The crystallite average size was calculated with Equation (1) for sample A_1 with diffraction plane (111), (200) and (211), and it was found to be 13.51 nm (Table 1). For sample A_2, diffraction plane (004), (200) and (211) was taken, the crystallite average size was 9.21 nm, and for sample A_3 was used the diffraction plane (111), (200) and (211). The crystallite average size was 13.91 nm. For all the samples, was calculated the crystalline average size from the crystalline phase.

One can see that all the samples show an amorphous phase, which indicates that temperature of heat treatment was not high enough to completely transform the amorphous phase to crystalline phase or heat treatment time was not long enough. It was also observed that the sample A_2, treated with hydrogen peroxide, was completely transformed into anatase phase. According to Sasirekha et al [26] the decrease in particle size can be attributed to the oxygen atom existing in the H_2O_2. During heat treatment the oxygen atoms were released from the particles which lead on the decrease of particle diameter. For the samples A_1 and A_3 the crystallites size was very close, which shows that the magnetic stirring do not influence the crystallites size. Powders with similar crystallite sizes were reported by Castro et al [11]. He obtained titanium dioxide powder with crystallites size between 12 ÷ 27 nm, using as precursor $TiCl_3$ in presence of ammonium hydroxide.

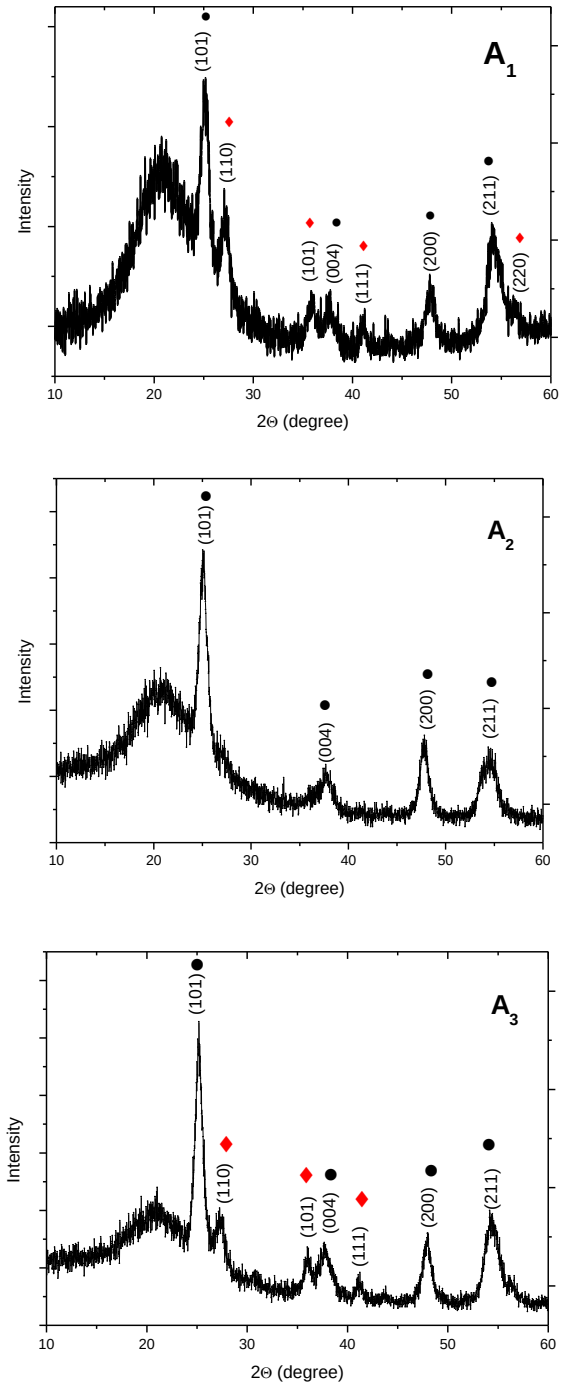

Fig. 1. XRD patterns of titanium dioxide samples after heat treatment at 500 ^{0}C, for 1 h: A_1 – static bath, A_2 - treatment with H_2O_2 30%, A_3 – magnetic stirring; ● - anatase, ♦ - rutile.

3.2. UV–Vis spectroscopic analysis

In Fig. 2 was presented the absorbance spectra of as prepared titanium hydroxide samples and the titanium dioxide obtained following heat treatment at 500 ^{o}C for 1h.

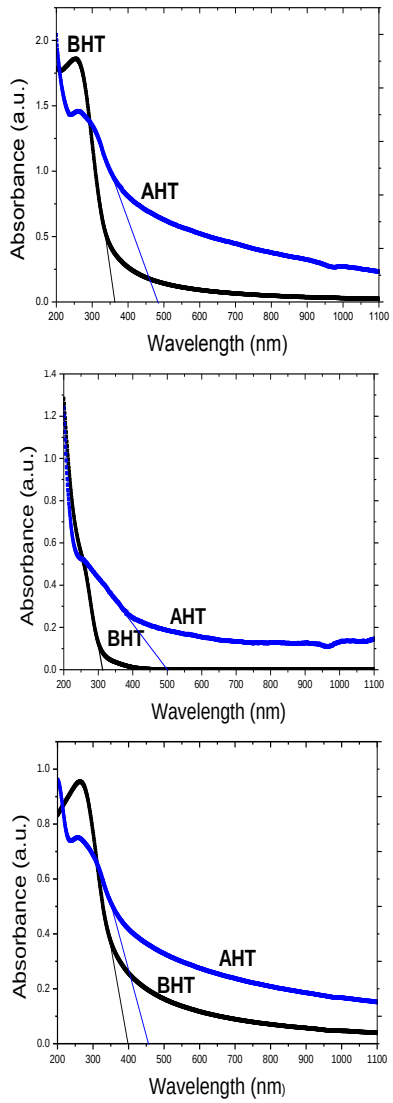

Fig. 2. Absorbance spectra for: a) sample A_1; b) sample A_2; c) sample A_3; before heat treatment (BHT), after heat treatment (AHT).

After heat treatment the shape of absorption spectra modify due to the transformation of titanium hydroxide in titanium dioxide, revealing absorption peaks at 262 nm for the sample A_1, at 259 nm for the sample A_2 and at 258 nm for the sample A_3. By heat treatment the amorphous titanium hydroxide converted to partially crystalline TiO_2 and the size of crystallites increases. According to Ge et al [27] the absorption peak of the TiO_2 shifts toward higher wavelengths by heat treatment. Another absorption peak is situated at wavelengths smaller than 200 nm for all samples.

The energy band gap, E_g, of the powders before and after heat treatment were determined using the absorption UV-Vis spectra. On the absorption curve slope was drew a line and then was read absorption wavelength of the sample. The optical energy band gap was calculated using the relationship [28]:

$$E_g = \frac{h \cdot c}{\lambda} = \frac{1240}{\lambda}$$

h – Planck's constant, h = 4.135×10^{-15} (eV·s), c - speed of light (m/s), c = 3×10^{8} (m/s), λ - wavelength of TiO_2 (nm).

Band gap can be also calculated with Tauc's low, by plotting $(\alpha h\nu)^n$ vs. (hν) and then by extrapolating the linear part of the curve to $(\alpha h\nu)^n = 0$ [10,29]. The relationship between the absorption coefficient α and incident photon energy (hν) can by written as:

$$(\alpha h\nu)^n = A(h\nu - E_g) \quad (3)$$

Where: α - the absorption coefficient, (hν) - photon energy, A – a constant which does not depend on photon energy, E_g - band gap energy, n – a constant, which depends on the type of transition. For indirect allowed transition n = ½, while for direct transitions n = 2. The plots of $(\alpha h\nu)^2$ for allowed direct transitions of TiO_2 powders versus photon energy are shown in Fig. 3 [30].

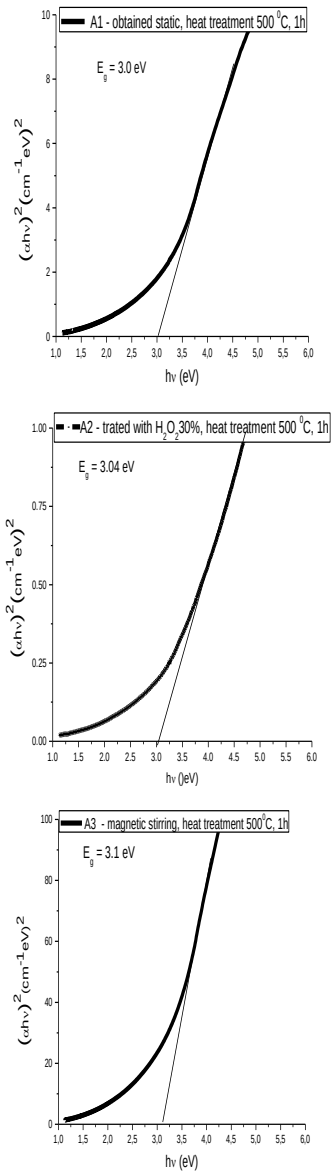

Fig. 3. The plot of $(\alpha h\nu)^2$ vs. (hν) of the samples A_1 obtained static at room temperature, A_2 treated with hydrogen peroxide 30%, and A_3 subjected to magnetic stirring. All the samples were subjected to heat treatment at 500 ^{0}C for one hour.

The obtained values for energy band gaps for TiO_2 powders, after heat treatment, determined with the absorption spectra and by plotting $(\alpha h\nu)^2$ vs. (hν) are presented in Table 2.

Table 2. Values for energy band gap after heat treatment for direct transition.

Sample	E_g determined from absorbance spectra [28] [eV]	E_g determined applying Tauc's low Direct band gap [eV]
A_1	2.48	3.00
A_2	2.23	3.04
A_3	2.72	3.10

One can see that the band gap of TiO_2 samples suffered a small decrease from the value corresponding to bulk TiO_2 for the both methods. A poor correlation between the estimated values for Eg using the two methods was noticed.

Because the most used and recognised method for Eg determination is the one based on Tauc law, we will take into consideration the values from column 3 from Table 2.

Comparing the values for E_g one can conclude that the obtaining conditions has a small influence on the band gap of the titania powders. The smallest value was obtained in the case of the sample obtained from static bath while the highest value correspond to the sample obtained under magnetic stirring. Solution mixing leads to a slight increase of crystallite size.

The small decrease of E_g comparing to the value corresponding to bulk material can be explained by the presence of chlorine in the titania network. EDS spectra (not presented) of samples obtained in conditions close to the conditions of the samples presented in this paper revealed the presence of chlorine. According with Long et al [24] and Rehman et al [31] chlorine doping introduces new levels in the band gap of titania, the energy for electron excitation in TiO_2 can be decreased and enables titania to absorb light with wavelengths as high as 400 nm.

In order to improve the response of TiO_2 powders a further decrease of Eg is necessary for obtaining response in visible region.

Even if the values obtained for E_g were high, the preliminary tests on the degradation of methylene blue revealed a good photocatalytic activity under solar radiation.

Nanostructured materials exhibit quantization effect. This is known as quantum size effect. This shows that there is a correlation between the increase of energy band gap of the semiconductor and the decrease of particle size. Quantization effect plays a vital role in controlling the photoelectrochemical and photocatalytic behaviour of semiconductors [2]. It is also well known that heat treatments lead to the increasing of crystallites size and to the decreasing of the energy band gaps of semiconductors [32,33,34]. One can suppose that an increasing of the treatment time could lead to smaller Eg due to the increasing of grain sizes.

4. Conclusion

TiO_2 nanocrystalline powder was successfully prepared using titanium trichloride as a precursor. By heat treatment at 500 ^oC, for 1 h, anatase and rutile crystalline phase of TiO_2 have been obtained both from static and magnetically stirred solutions. The treatment with H_2O_2 of sample A_3 leads to the formation of anatase (photoactive phase) alone. Energy band gaps slightly decreased for all the samples from the value of bulk titania (from 3.2 eV to 3 – 3.1 eV). It was assumed that the slight decrease of energy band gap was caused by chlorine from precursor solution used in preparing of titanium dioxide powder. After heat treatment we suppose that chlorine entered into TiO_2 network playing a pole of a dopant. This theory will be discussed in our next paper. A poor correlation between the grain size determined by X ray diffraction and the band gap has been noticed.

Acknowledgments

This paper was supported by the project "Doctoral studies in engineering sciences for developing the knowledge based society-SIDOC" contract no. POSDRU/88/1.5/S/60078, project co-funded from European Social Fund through Sectorial Operational Program Human Resources 2007-2013.

Authors thank Prof. phD. Eugen Culea and Asist. Prof. phD. Petru Păşcuţă for assistance in XRD measurements.

References

[1] M. Behpour, S. M. Ghoreishi, F. S. Razavi, Digest Journal of Nanomaterials and Biostructures **5**, 467 (2010).
[2] S. Janitabar-Darzi, A. R. Mahjoub, A. Nilchi, Journal Physica E **42**, 176 (2009).
[3] N. M. Tuan, N. T. Nha, N. H. Tuyen, Journal of Physics: Conference Series **187**, (2009).
[4] S. K. Sharma, M. Vishwas, K. N. Rao, S. Mohan, D. S. Reddy, K. V. A. Gowda, Journal of Alloys and Compounds **471**, 244 (2009).
[5] I. Zumeta, B. Gonzalez, R. Espinosa, J. A. Ayllon, E. Vigil, Juranlul Semicond. Sci. Technol. **19**, 52 (2007).
[6] E. Vigil, D. Dixon, J. W. J. Hamilton, J. A. Byrne, Surface & Coatings Technology **203**, 3614 (2009).
[7] H. Sun, C. Wang, S. Pang, X. Li, Y. Tao, H. Tang, Journal of Non-Crystalline Solids **354**, 1440 (2008).
[8] T-C. Cheng, K-S. Yao, Y-H. Hsieh, L-L. Hsieh, C-Y. Chang, Materials and Design, (2009).
[9] C. Giolli, F. Borgioli, A. Credi, A. Di Fabio, A. Fossati, M. M. Miranda, S. Parmeggiani, G. Rizzi, A. Scrivani, S. Troglio, A. Tolstoguzov, A. Zoppi, U. Bardi, Surface & Coatings Technology **202**, 13 (2007).
[10] C. K. Lee, D. K. Kim, J. H. Lee, J. H. Sung, I. Kim, Journal of Sol-Gel Science and Technology **31**, 67 (2004).
[11] A. L. Castro, M. R. Nunes, A. P. Carvalho, F. M. Costa, M. H. Florencio, Solid State Sciences **10**, 602 (2008).
[12] S. Cassaignon, M. Koelsch, J-P Jolivet, Journal of Physics and Chemistry of Solids **68**, 695 (2007).
[13] Y. Zhiyong, E. Mielczarski, J. Mielczarski, D. Laub, Ph. Buffat, U. Klehm, P. Albers, K. Lee, A. Kulik, L. Kiwi-Minsker, A. Renken, J. Kiwi, Water Research **41**, 862 (2007).
[14] X. Zhao, Z. Li, Y. Chen, L. Shi, Y. Zhu, Journal of Molecular Catalysis A: Chemical **268**, 101, (2007).
[15] Q. Tang, J. Lin, Z. Wu, J. Wu, M. Huang, Y. Yang, European Polymer Journal **43**, 2214 (2007).
[16] Y. Zhu, S. Xu, D. Yi, Reactive & Functional Polymers **70**, 282 (2010).
[17] D. Wanga, J. Zhanga, Q. Luob, X. Lib, Y. Duana, J. Anb, Journal of Hazardous Materials **169**, 546 (2009).
[18] Y. Zhu, Y. Dan, Solar Energy Materials & Solar Cells, 2010.
[19] R. A. Damodar, S-J You, H-H Chou, Journal of Hazardous Materials **172**, 1321 (2009).
[20] L. Andronic, A. Enesca, C. Vladuta, A. Duta, Chemical Engineering Journal **152**, 64 (2009).
[21] M. A. Barakat, G. Hayes, S. Ismat Shah, Journal of Nanoscience and Nanotechnology**10**, 1 (2005).
[22] N. Bao, Z. Wei, Z. Ma, F. Liu, G. Yin, Journal of Hazardous Materials, (2009).
[23] G. Li, C. J. Yu, D. Zhang, X. Hu, W. M. Lau, Separation and Purification Technology **67**, 152 (2009).
[24] M. Long, W. Cai, H. Chen, J. Xu, Front. Chem. China **2**, 278 (2007).
[25] Y. B. Zhang, X. J. Feng, L. Jiang, Sci China Ser B-Chem **50**, 175 (2007).
[26] N. Sasirekha, B. Rajesh, Y-W Chen, Thin Solid Films **518**, 43 (2009).
[27] L. Ge, M. Xu, H. Fang, Thin Solid Films **515**, 3414 (2007).
[28] K. Porkodi, S. Daisy Arokiamary, Materials Characterization **58**, 495 (2007).
[29] P. Dennis Christy, N. S. Nirmala Jothi, N. Melikechi, P. Sagayaraj, Cryst. Res. Technol. **44**, 484 (2009).
[30] L. Zhao, J. G. Yu, J. Colloid Interface Sci. **304**, 84 (2006).
[31] S. Rehman, R. Ullah, A. M. Butt, N. D. Gohar, Journal of Hazardous Materials **170,** 560 (2009).
[32] L. C. Andronic, Nanostructured ceramic materials with photocatalytic properties used for water pollutants degradation, Brasov, 2010.
[33] A. M. More, T. P. Gujar, J. L. Gunjakar, C. D. Lokhande, O-S Joo, Applied Surface Science **255**, 6067 (2008).
[34] B. Yarmand, S.K. Sadrnezhaad, J. Optoelectron. Adv. Mater. **12**, 1490 (2010).

*Corresponding author: violeta.popescu@chem.utcluj.ro